A Practical Method of Image Enhancement by Interactive Digital Filtering

Tom R. Miller and Edward S. Rollins*

The Edward Mallinckrodt Institute of Radiology, Washington University School of Medicine, St. Louis, Missouri

A generalized form of the Wiener digital filter is described in which the user interactively varies two filter parameters to produce any desired number of filtered versions of a given image with differing blends of sharpening and smoothing qualities. Filtering is performed sufficiently rapidly, even without use of an array processor, to make application of the filter truly interactive. Use of the filter is illustrated with typical nuclear medicine images.

The Wiener and closely-related Metz digital filters have been shown to improve image quality and facilitate interpretation of nuclear medicine images (*1–4*). Past work with these filters was based on a close matching of the filter to the characteristics of each type of image, principally through determination of camera blur by way of the modulation transfer function (MTF) and measurement or estimation of the signal-to-noise ratio (SNR). When filtering of a wide range of nuclear medicine images is desired, this precise matching of a particular filter to each image becomes difficult because of the multiplicity of factors determining the MTF and SNR for the different images. Furthermore, the matching of filter characteristics to a given image leads to generation of a single "optimal" filtered image. In many situations it may be desirable to produce several filtered versions of a particular image with differing sharpening and smoothing properties.

Therefore, to overcome the problems associated with the multiplicity of different images and to provide a range of filtered representations of each image, we have developed an interactive filtering method retaining the functional form of the Wiener filter. With this technique the user can sit at a video terminal and rapidly and interactively vary the basic filter parameters to generate any desired number of filtered versions of the image under analysis.

MATERIALS AND METHODS

Wiener filter theory

The Wiener filter has been described in detail previously (*1,2,5–7*). Briefly, this filter generates an image such that the mean-square-error between the undegraded source distribution and the filtered image is minimized. For filtering performed in the frequency domain (*5,8*), the Fourier transform of the filtered image $I'(f)$ is the product of the Fourier transform of the original image $I(f)$ and the filter transfer function $H(f)$:

$$I'(f) = I(f) \cdot H(f) \qquad (1)$$

where f is the spatial frequency (represented, for notational simplicity, in one dimension). The filtered image in the spatial domain (X-Y coordinates) is then obtained as the inverse transform of $I'(f)$. For the Wiener filter

$$H(f) = \frac{MTF(f)}{(MTF(f))^2 + 1/SNR(f)} . \qquad (2)$$

The SNR may be expressed as

$$SNR(f) = P_o(f)/P_n(f) \qquad (3)$$

where P_o is the power spectrum of the object (before degradation by blur and noise) and P_n is the power spectrum of the
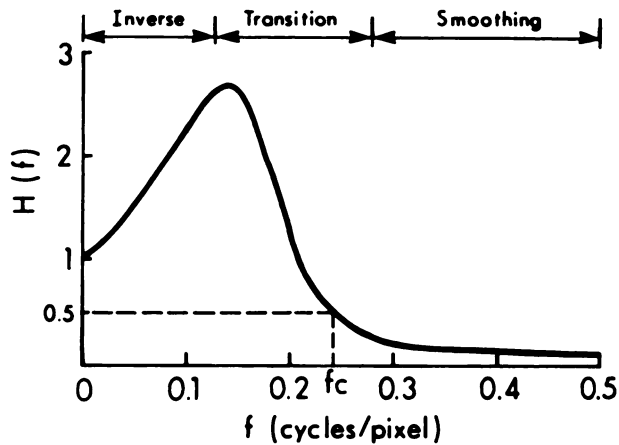
FIGURE 1
Filter transfer function H(f) is shown for typical Wiener filter. Inverse filter, transition, and smoothing regions are shown

FIGURE 2
Three Wiener filters are shown with widely differing sharpening and smoothing properties. Filter A is very strong sharpening filter with long, steep inverse filter region ($f_{1/2}$ = 0.08, f_c = 0.40, N = 200,000). Filter B is intermediate, with moderate sharpening and smoothing qualities ($f_{1/2}$ = 0.16, f_c = 0.33, N = 200,000). Filter C is heavy smoothing filter with negligible sharpening ($f_{1/2}$ = 0.44, f_c = 0.17, N = 200,000)

noise. Goodman and Belsher (6), employing a Poisson noise model, developed an expression relating P_o to the power spectrum of the actual observed image. They also determined that P_n is independent of frequency and equal to the total number of counts in the image. These theoretical results were confirmed by King et al. in measurements performed on a variety of nuclear medicine images (2). They found that $P_c \gg P_n$ for spatial frequencies below some cutoff frequency fc and $P_o \ll P_n$ for frequencies greater than fc. Therefore, Eq.(2) reduces to the following:

$$H(f) \approx \begin{cases} 1/MTF(f) & (f \ll f_c) \\ MTF(f)/(MTF(f)^2 + 1/SNR(f)) & (f \approx f_c) \\ 0 & (f \gg f_c) \end{cases}$$

(4)

In the transition region near fc, a log-exponential fit to King's data for $P_o(f)$ is employed with adjustment of parameters such that H(fc) = 0.5 (see Appendix).

Generalization of the theory

The expression for the Wiener filter given in Eq. (4) leads to a generalized form of the filter consisting of three components corresponding to the frequency regions in the equation (see Fig. 1). The first, low-frequency part is an inverse filter where

$$H(f) = 1/MTF(f).$$

(5)

In this frequency region, the blurring introduced by the scintillation camera, and expressed through the MTF, is corrected for by multiplying the image by the reciprocal of the MTF leading to "resolution recovery" or image sharpening (9). To prevent unacceptable artifacts in regions of low SNR, the inverse filter must be rolled off to zero giving a low-pass or "smoothing" property to the filter with suppression of high frequencies:
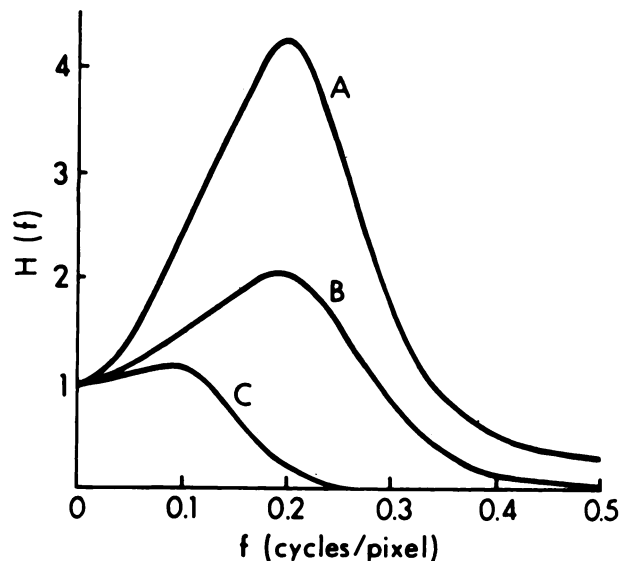
$$H(f) \approx 0 \quad (f \gg f_c) \tag{6}$$

where f_c characterizes the smoothing quality of the filter. As seen from Eq. (4) there is a transition band between the two forms where $f \approx f_c$ (see Appendix).

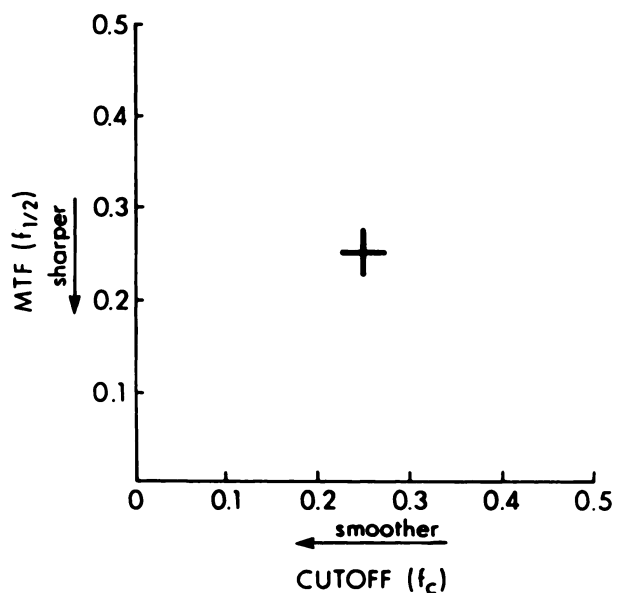The blending of these sharpening and smoothing properties

FIGURE 3
Operator interactively positions cursor on this graph to select sharpening and smoothing parameters $f_{1/2}$ and f_c

TABLE 1
Time Required to Filter an Image

Image size (pixels)	Processing time (sec)		
	PDP-11	VAX	AP
64 × 64	1.8*	1.1	0.12†
128 × 128	12‡	4.3	0.20§

* Time is less than given in Ref. *10* because of greater use of assembly language programming.

† Ref. *10*.

‡ Extrapolated from the VAX measurements based on relative processor speeds and time required to segment arrays on PDP-11.

§ Ref. *11*.

of the Wiener filter leads to a generalized form with two adjustable parameters—one controlling the sharpening and one the smoothing. To adjust the sharpening property for our particular data, the MTF was found to best approximate an exponential function:

$$MTF(f) = \exp(-f/f_o) = 2^{-f/f_{1}/2} \qquad (7)$$

where f_o or $f_{1/2}$, the first adjustable parameter, determines the rate of decline of the MTF with frequency, and therefore, the slope of the inverse filter. The smoothing is controlled by adjustment of the transition, or cutoff, frequency f_c. Thus, variation of the parameters $f_{1/2}$ and f_c leads to the generation of a large family of filters with a continuously variable mix of sharpening and smoothing qualities (see Fig. 2).

Implementation

As previously described in detail (*5,8*), digital filtering can be performed either in the frequency domain, with use of the fast Fourier transform (FFT), or in the spatial domain, employing finite-impulse-response (FIR) filters. We chose the FIR approach because of lack of computational pitfalls including wraparound error and leakage (*5*) and because of the availability of the very fast Chebyshev algorithm (*10*) to perform the convolutions. The Chebyshev algorithm is faster

than the FFT method even for very large FIR filter sizes (~51 × 51 pixels), and the Chebyshev approach gives results mathematically identical to those achieved with direct convolution. If an array processor is available, the FFT method may be preferred because of greater speed of frequency-domain filtering on the array processor (*10*). We selected a mask size of 11 × 11 pixels, leading to errors in the frequency response of the filters of only 3–5%.

Interactive selection of the filter variables is achieved through display of a graph on a video monitor with $f_{1/2}$ and f_c as the ordinate and abscissa, respectively (Fig. 3). The operator selects the values of these two variables by movement of a joystick-controlled cursor to the desired position on the graph. One of 100 pre-computed FIR filters, stored in the filter program, is then selected according to the cursor position. If frequency-domain filtering is employed, the filter transfer function is quickly computed from Eqs. (4)–(7) after cursor positioning.

The computations are performed on a PDP-11/34a* or VAX-11/750* computer with use of programs written partly in FORTRAN and partly in assembly language. Alternatively, computation can be performed with use of an array processor.

Images are collected in 128 × 128 pixel arrays, except for gated cardiac blood-pool scans and dynamic studies which are collected in 64 × 64 pixel format. High-quality video systems with 256 gray-shade capability are used for image display and analysis.

Applications

This interactive Wiener filter is used with all types of nuclear medicine images. To illustrate the performance of the filter, typical results are shown for thyroid, bone, and renal scans.

RESULTS

The time required to filter 64 × 64 pixel and 128 × 128 pixel images, exclusive of minimal disc I/O, is shown in the
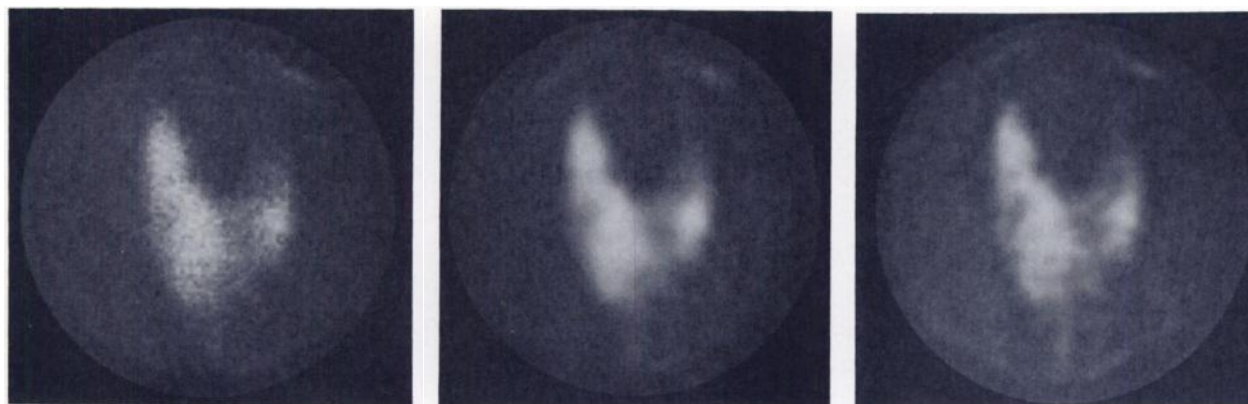

FIGURE 4
169,000 count image from [99mTc]pertechnetate thyroid scan is shown. Study was collected on large-field-of-view camera equipped with pinhole collimator. Unfiltered image is at left, while filtered image obtained with use of soft filter is shown in center ($f_{1/2}$ = 0.32, f_c = 0.16, N = 169,000), and more sharply filtered image is at right ($f_{1/2}$ = 0.15, f_c = 0.22, N = 169,000)
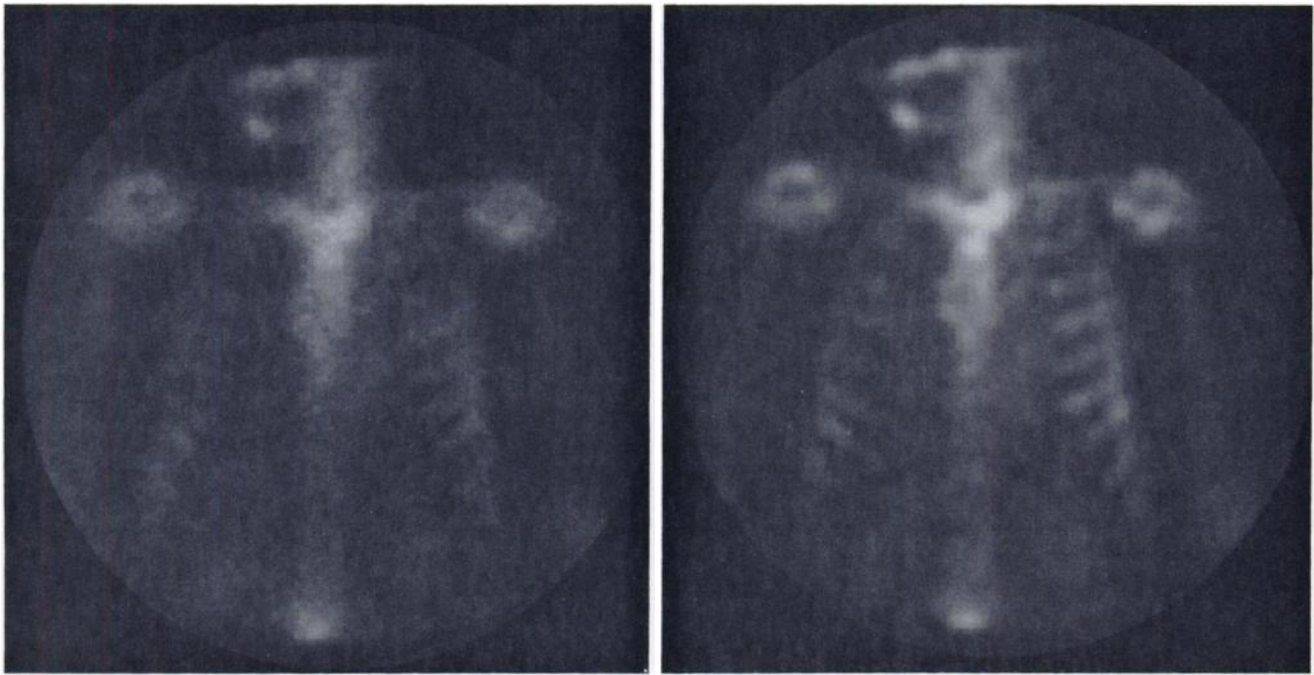
FIGURE 5
600,000 count image from bone scan is shown. Study was collected on large-field-of-view camera equipped with an all-purpose, parallel-hole collimator. Unfiltered image is shown on left with filtered image on right. Filter is very similar to filter B in Fig. 2 ($f_{1/2}$ = 0.15, f_c = 0.29, N = 600,000). Note significant increase in rib detail with use of Wiener filter

table for FIR filtering on the PDP-11/34a and VAX-11/750 computers and FFT filtering by an array processor[†]. While the time is least with use of the array processor, computation speed is, nevertheless, entirely satisfactory without the array processor to achieve the goal of user-interactive filtering.

Figures 4, 5, and 6 show, respectively, typical unfiltered and filtered images from a thyroid scan, a bone scan, and a technetium glucoheptonate renal flow study.

DISCUSSION

The Wiener and closely-related Metz filters have been applied to a wide range of nuclear medicine images (1-4). As the number of nuclear medicine departments with all-digital image acquisition and analysis increases, there is a need for a general-purpose filter
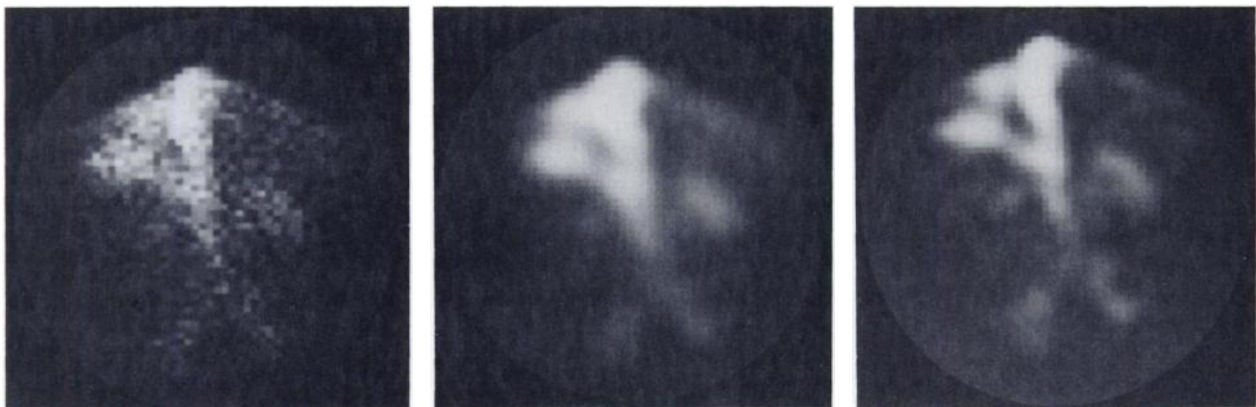

FIGURE 6
5,000 count image from technetium glucoheptonate renal flow study is shown. This is 1-sec frame collected in posterior projection on large-field-of-view camera equipped with high-energy, parallel-hole collimator. Unfiltered image is shown at left, while filtered image obtained with use of soft filter is shown in center ($f_{1/2}$ = 0.30, f_c = 0.20, N = 5,000), and more sharply filtered image is at right ($f_{1/2}$ = 0.22, f_c = 0.28, N = 5,000). Note greater vascular and renal detail achieved with both filters in this patient with poorly perfused left kidney

applicable to all images. Past work with the Wiener filter has relied on precise matching of the filter to the characteristics of a particular image. In the work reported here, the basic form of the Wiener filter has been generalized while retaining the filter's salient property of image sharpening coupled with noise suppression. A very important feature of this new method is the interactive, operator-controlled blending of the filter's sharpening and smoothing qualities. Thus, the user, sitting at a video display, can quickly generate any desired number of filtered versions of the images under study to bring out different features of the images or analyze suspected abnormalities with use of widely-differing filtered images. This process is similar in operation to the popular technique of interactive variation of gray level, but it is on a completely different computational plane.

To make the use of this filter truly interactive, the filtering operation must be rapid and selection of the desired filters must be quick and convenient. As shown in the table, filtering is sufficiently fast, even without an array processor, to achieve the desired interactive quality. The joystick-controlled method of filter selection, shown in Fig. 3, is very quick and easy to use.

Experience with these filters has shown that high count, high contrast images are improved most with use of strong filters with significant sharpening (see the bone scan in Fig. 5). Images with intermediate contrast and counts as well as low count, high contrast images may benefit from either smoothing or sharpening (Figs. 4, 6). Weaker filters with only moderate sharpening and significant smoothing properties are most effective with low count (low SNR) images with low contrast.

As with any filtering method, artifacts can be produced which could lead to incorrect image interpretation. With this filtering technique the greatest artifacts occur when too strong a filter is selected. A mottled, patchy pattern can be generated which could suggest inhomogeneous activity in uniform regions (note the background areas in Figs. 4 and 6). This artifact is recognized by inspection of these regions after processing by weaker filters and by frequent reference to the unfiltered images.

No attempt has been made here to prove the diagnostic value of this interactive filtering technique. However, judicious application of these filters is likely to improve image interpretation in many cases, as has been demonstrated for noninteractive versions of the Wiener and related filters applied to several types of nuclear medicine images (1-4).

FOOTNOTES

* Digital Equipment Corporation, Maynard, MA.
† AP-400, Analogic Corporation, Wakefield, MA.

APPENDIX

The power spectrum P_0 of the undegraded object can be determined from the power spectrum of the observed image P_i with use of the expression

$$P_0(f) = (P_i(f) - N)/(MTF(f))^2, \qquad (A1)$$

where N is the total number of counts in the image (2,6). King et al. (2) measured P_i for a wide range of nuclear medicine images. Their data may be approximated by a log-exponential function

$$\log P_i(f) = a(\exp(-kf)-1) + \log N, \qquad (A2)$$

where a and k are constants determined by the data. Since P_n = N (2,6), the expression for SNR given in Eq. (3) may be written as

$$\begin{aligned} SNR &= P_0/P_n \\ &= MTF^{-2} (\exp(a(\exp(-kf)-1)))/N. \quad (A3) \end{aligned}$$

Most image data are fit well with a = 7. The cutoff frequency f_c used in Eqs. (4) and (6) is chosen such that $H(f_c) = 0.5$. This requirement serves to determine k in Eq. (A3). If desired, the exact value of N may be selected for each type of image, although this is usually not necessary since the precise value of SNR has only a subtle effect on H(f) in the transition region near $f = f_c$ and no effect in the inverse and smoothing regions.

REFERENCES

1. Miller TR, Goldman KJ, Epstein DM, et al: Improved interpretation of gated cardiac images by use of digital filters. *Radiology* 152:795-800, 1984
2. King MA, Doherty PW, Schwinger RB, et al: A Wiener filter for nuclear medicine images. *Med Phys* 10:876-880, 1983
3. King MA, Miller TR, Jacobs DA, et al: Nonstationary image processing in the frequency domain. In *Digital Imaging, Clinical Advances in Nuclear Medicine*, New York, The Society of Nuclear Medicine, 1982, pp 127-141
4. King MA, Doherty PW, Schwinger RB, et al: Fast count-dependent digital filtering of nuclear medicine images: Concise communication. *J Nucl Med* 24:1039-1045, 1983
5. Miller TR, Sampathkumaran KS: Digital filtering in nuclear medicine. *J Nucl Med* 23:66-72, 1982
6. Goodman JW, Belsher JF: Fundamental limitations in linear invariant restoration of atmospherically degraded images. *Proc SPIE* 75:141-154, 1976
7. Hart RW, Farrell RA: Image distribution of radioactivity within the human body. I. Theoretical considerations in optimum data processing. *Invest Radiol*

3:199-212, 1968

8. Miller TR, Sampathkumaran KS: Design and application of finite impulse response digital filters. *Eur J Nucl Med* 7:22-27, 1982

9. Pratt WK: *Digital Image Processing,* New York, John Wiley and Sons, 1978, pp 378-381

10. Miller TR, Sampathkumaran KS, King MA: Rapid digital filtering. *J Nucl Med* 24:625-628, 1983

11. King MA, Doherty PW, Rosenberg RJ, et al: Array processors: An introduction to their architecture, software, and application in nuclear medicine. *J Nucl Med* 24:1072-1079, 1983